

# Vertical Cosine Response of a Faired Ring Acoustic Current Meter

Albert J. Williams 3<sup>rd</sup>  
Woods Hole Oceanographic Inst.  
Woods Hole, MA 02543 USA  
[awilliams@whoi.edu](mailto:awilliams@whoi.edu)

Archie Todd Morrison III  
Nobska Development, Inc.  
Woods Hole, MA 02543 USA  
[atmorrison@nobska.net](mailto:atmorrison@nobska.net)

Samantha R. Brody  
Swarthmore College  
Swarthmore, PA 19081 USA  
[samib23@gmail.com](mailto:samib23@gmail.com)

**Abstract** - Measurement of current in the horizontal plane requires that the azimuth of the fluid velocity vector projected onto the horizontal plane be accurately represented in Cartesian coordinates with a cosine response in the x and y direction. In the acoustic current meter that was studied, MAVS (Modular Acoustic Velocity Sensor, Nobska Development, Inc.), the horizontal cosine response is excellent, varying from ideal by less than 5%.

When a full vector current measurement is made, there is a further requirement that the projection of the fluid velocity vector onto the vertical or z axis have a cosine response to the elevation angle of the velocity vector. Structures supporting the acoustic transducers in an acoustic current meter necessarily create wakes and distort the flow. Minimizing this disturbance through faired supports improves the vertical cosine response; however, there remains a velocity defect of as much as 20% for flows exceeding a 45° elevation angle in MAVS. For flows elevated less than 30° from the horizontal plane, the deviation from ideal cosine response is less than 10% and over a 50° range in elevation angle the deviation from ideal cosine response is less than 5%.

## I. INTRODUCTION

Measurements of fluid velocity from an acoustic travel-time current meter require acoustic transducer supports that form the ends of the acoustic path along which the measurement is made [1]. The wake of these supports decreases the velocity close to the transducers and can cause the differential travel-time of the acoustic signal to underestimate the free-fluid velocity. Acoustic paths that are oblique to the flow direction minimize this effect because the wake is mostly outside the path. However, as a fully three-dimensional flow instantaneously falls along the acoustic path direction or when an acoustic axis is purposely aligned with the flow, the wake decreases the velocity that is measured from that of the free-stream and the measurement underestimates the flow that would be present without the transducer supports. The velocity attenuation of a wake from a fixed direction can be calibrated and corrections applied in steady flow, but the variations of this attenuation with direction can be complex and the wake itself may be turbulent or the flow itself may be unsteady so that the attenuation in velocity component along the acoustic path can be time varying. In 1994, the solution of fairing the support structures, rings, to minimize the wake when the flow was along an acoustic axis was implemented in the new current sensor, MAVS [2]. This both reduced the velocity defect in the wake where it occupied a significant portion of the acoustic measurement axis and reduced the unsteadiness of the wake so that the velocity measured was less contaminated with time variations than it might have been without fairing.

## II. HARDWARE

### A. Faired Rings

Acoustic transducers used in travel-time velocity measurements are directional and ultrasonic, resonant at the frequencies used for the measurement, typically about 2 MHz. This imposes a thickness for the piezoceramic elements of about 1 mm. The diameter of the transducers affects acoustic beam width and thus sensitivity. Too large a diameter may produce a beam width so narrow that the alignment error in normal assembly and use may reduce the signal below what might have been experienced in a smaller transducer with a wider beam width. In MAVS, the compromise was a 10 cm path length and 3 mm by 8 mm rectangular transducers. The resonant frequency of 1.8 MHz yields a beam width of 16° by 6° with the wide beam width ensonifying the long dimension of the receiving transducer. In each case, the beam width is about three times the physical dimension of the transducer, ensuring that the receiving transducer is uniformly ensonified by the transmitting transducer. The transducers can be seen below their epoxy coverings in Figs. 1 and 2.

The narrow dimension of the transducer, 3 mm, can be buried in the 4.5 mm cross-sectional thickness of the faired ring. The over molding of the transducer and the machined flats of the ring to which the transducers are glued with epoxy and fiberglass increases the thickness in the region of the transducer itself to about 8 mm for approximately 20 mm of the circumference of the ring. As the flow approaches the direction of the acoustic path, the projected area of the ring decreases until it is minimized along the path direction. But fairing also reduces the velocity defect of the wake through a reduction of drag coefficient, by up to a factor of 10 over a bluff body.

Fairing adds volume to the ring so in directions other than along the faired direction, the projected area is greater than it would be without fairing. Fairing is absent directly in front of the transducer because acoustic refraction in the extra material would attenuate the acoustic signal below an acceptable level. However on either side of the transducer the fairing increases the depth of the ring to 13 mm. The struts that connect the faired ring to the central supporting tube (12.5 mm in diameter) connect to the rings 45° around the circumference from the transducers so that when the flow lies close to an acoustic axis, the flow in the measurement volume is unaffected by the wake from the struts. Finally, the rings shed a cylindrical or ellipsoidal sheet wake. A cord in this cylinder such as an acoustic path intersects the sheet in only two small regions, except when the flow is directly along an acoustic path.



Fig. 1. MAVS velocity sensor. The faired rings are 118 mm in diameter, separated by 70 mm, each supported by four struts from a central support tube 12.5 mm in diameter. This view is that seen by flow at 0° elevation



Fig. 2. Velocity sensor viewed on axis. This is a bent sensor showing the struts supporting the rings but the housing is off to the left. This view is that seen by the flow at 90° elevation.

### B. Projected Area

For horizontal flow, the projected area of each ring is  $10.5 \text{ mm} \cdot 118 \text{ mm}$  or  $1240 \text{ mm}^2$  with additional structural area outside the ensounded volume presented

by struts of a conical shape, 12 mm high and 118 mm in diameter or  $708 \text{ mm}^2$ , for a total of  $1950 \text{ mm}^2$ . Within the ensounded volume there is also a central supporting tube as shown in Fig. 1 with a width of 12.5 mm and the length between the two rings of 70 mm. Adding all of these projected areas together the structural area of the sensor is  $4770 \text{ mm}^2$  over a total cross sectional area of the sensor of  $16,040 \text{ mm}^2$ . Thus the total opacity of the sensor for horizontal flow is 30% where opacity is the projected area of the structure divided by the total area.

The total projected area for horizontal flow is most useful for determining the drag of the sensor and this in turn is responsible for a total deceleration of the flow in the wake region of the sensor. However, the details of the flow that crosses the measurement path are important for understanding the accuracy of the measurement, and the structural elements that are upstream of the acoustic path are more significant for that than those that are downstream. Projected area for horizontal flow is just such an estimate since the first structure that the flow encounters is the upstream part of the ring. But even here, the flow splits around the ring and the portion of the flow that diverges above the upper ring or below the lower ring and then encounters the struts forming a conical structure is less relevant to the measurement than the part of the flow that diverges into the volume between the rings. A more appropriate estimate of the opacity seen by the measured part of the flow would be half of the projected area of the rings and the section of central supporting tube that is between the rings. The half ring area is  $\frac{1}{2} \cdot 10.5 \text{ mm} \cdot 118 \text{ mm}$  or  $620 \text{ mm}^2$ , the central supporting tube area is  $12.5 \text{ mm} \cdot 70 \text{ mm}$  or  $875 \text{ mm}^2$ , for a total projected area of structure encountered by the measured flow of  $2110 \text{ mm}^2$ . The total area between the separation lines of the rings is  $118 \text{ mm} \cdot (70 \text{ mm} + 10.5 \text{ mm})$  or  $9500 \text{ mm}^2$ . This gives opacity of 22% for the measured portion of horizontal flow.

For purely vertical flow or flow in-line with the sensor axis, the projected area of a single ring is  $\pi \cdot 118 \text{ mm} \cdot 8.5 \text{ mm}$  or  $3150 \text{ mm}^2$ . The struts add  $4 \cdot 5 \text{ mm} \cdot 48.5 \text{ mm}$  or  $970 \text{ mm}^2$ . The central tube with hub molding adds a circular cross section of  $\pi \cdot (21 \text{ mm}/2)^2$  or  $346 \text{ mm}^2$ . The total projected area of the structure along the sensor axis is thus  $4466 \text{ mm}^2$  out of a total area of  $\pi \cdot (118 \text{ mm}/2)^2$  or  $10,940 \text{ mm}^2$ . This projects a total opacity of the sensor in this direction of 41%. This does not include the second ring with its struts and the central tube because these are behind the first ring and struts. This shadowing is not accurate in a flow where the rings are separated by 70 mm. If both rings and struts but not the central tube were included, the projected area would be  $8586 \text{ mm}^2$  and the opacity in the along sensor axis direction would be 78%. While this second projected area may be important for the drag of the sensor volume to flow in this direction and to the total flow deceleration for flow passing through the sensor volume, it is only the first that is relevant to the measurement accuracy since the second ring is downstream of the acoustic paths along which the flow is measured. The sensor viewed on axis is shown in Fig. 2.

If the flow is tilted so that it falls between horizontal and purely vertical, the projected area will increase from the purely horizontal flow case as more of the flow that enters the measurement volume encounters the struts supporting the ring that is upstream and the separation line moves from the equator of the ring towards its upper edge. The length of ring that is projected becomes an arc instead of a straight line and approaches a full circle with increasing azimuthal angle.

On the other hand, the projected section of the ring thins from 10.5 mm to 4 mm as the elevation angle approaches 45°. While the far side of each ring comes out from the shadow of the near side of the ring, this only affects the total drag of the sensor since these structural elements are downstream of the acoustic paths along which the velocity is measured. Fig. 3 shows the sensor for an elevation of about 15°. The effective projected area of a tilted ring is hard to compute and the assumption that the projected area is the critical quantity for flow obstruction is an approximation, so we proceeded to measure the response to flow for a tilted sensor.



Fig. 3. MAVS velocity sensor for an elevation of about 15°. The acoustic paths are only shadowed by one of the upper struts, a short section of the upper ring, and the central support tube.

### C. Volume of Sensor Structure

When a structure becomes moderately opaque, the projected area is not the only measure of flow obstruction and the relative volume of structure to total volume is revealing. The volume of the ring is approximately  $\pi \cdot 118 \text{ mm} \cdot 12 \text{ mm} \cdot 4 \text{ mm}$  or  $18,790 \text{ mm}^3$ . The volume of the struts is

$4 \cdot 42 \text{ mm} \cdot 11 \text{ mm} \cdot 5 \text{ mm}$  or  $9,240 \text{ mm}^3$ . The volume of the hub at each ring is  $\pi \cdot (21 \text{ mm}/2)^2 \cdot 25 \text{ mm}$  or  $8660 \text{ mm}^3$ . The support tube between the rings is  $\pi \cdot (12.5 \text{ mm}/2)^2 \cdot 70 \text{ mm}$  or  $8590 \text{ mm}^3$ . Thus the total support structure within the volume is  $81,970 \text{ mm}^3$ , which is 9.4% of the total enclosed volume of  $874,900 \text{ mm}^3$  ( $\pi \cdot (118 \text{ mm}/2)^2 \cdot (70 \text{ mm} + 2/3 \cdot 15 \text{ mm})$ ).

The velocity inside the sensor volume is reduced by the fixed structure but there is also acceleration of the velocity near a structure and, in fact, the velocity measured along an acoustic path with the flow in the horizontal plane is very close to the calculated value with no velocity defect.

### D. Acoustic Axis

The principle of the acoustic travel-time measurement of velocity is that sound travels through fluid at the group velocity of the sound relative to the fluid so that a pulse of sound transmitted from the left transducer to the right transducer travels at the velocity  $c$  plus the component of flow along the transducer axis,  $u \cos(\theta)$  where  $c$  is the speed of sound,  $u$  is the speed of the fluid, and  $\theta$  is the angle between the acoustic axis and the velocity vector. Sound traveling from right transducer to the left transducer moves at  $c$  minus  $u \cos(\theta)$ . The difference in the two travel times,  $\Delta t$ , is  $2 L u \cos(\theta)/c^2$  where  $L$  is the distance between the transducers. This is shown schematically in Fig. 4. A more accurate formulation is a line integral along the acoustic path of each element of velocity, angle, and distance so that the travel-time difference is an average of the velocity distribution along the path in the direction of the acoustic transmission. An even more accurate formulation is to evaluate a Fresnel integral describing the propagation of sound through the water, but this considerably more complex approach “collapses” to the path integral in actual practice [3, 4]. The point here is that there is a region of stagnant water just in front of the transducer but out a short distance the fluid is accelerated by the structure and compensates in part for the velocity lost in the near field [4, 5].

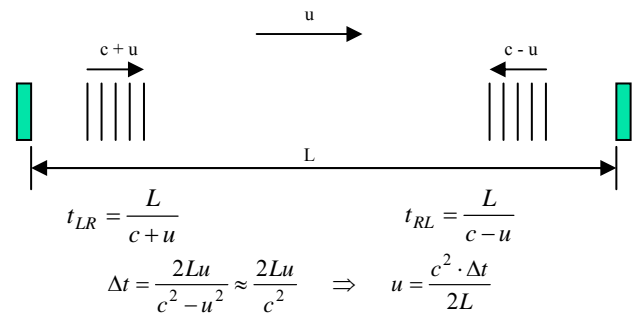


Fig. 4. Acoustic travel-time measurement of flow derives from the sound propagating through the fluid at the group velocity of sound with respect to the moving fluid.

Four paths are used in MAVS, each spaced 90° in azimuth around the sensor and inclined 45° to the plane of the rings so that for horizontal flows, the wake of the rings is largely away from the acoustic paths. When the flow leaves the horizontal plane this relative immunity

from wake effects is reduced. Experiments in 1995 showed that the vertical response of the sensor in MAVS also followed the cosine law of the formulation within 15% [6] but measurements were only made every 15° in elevation. Based upon this favorable result, the shape of the rings was kept and MAVS sensors have been made to this design since that time with only slight changes in the hub moldings where the rings meet the support tube.

### III. TOW TANK TESTS

#### A. Tow Tank

Calibration of velocity sensors requires a known flow against which the readings of the sensor can be compared [7]. At Woods Hole Oceanographic Institution, a 20 m tank has been equipped with a precise tow carriage for this purpose. The tank is 1.2 m wide and 1 m deep. The carriage runs on rails above the tank and is driven by a stepping motor for speeds up to 90 cm/s under computer control. Start up time depends on speed but is typically less than 2 seconds. The tank is filled with fresh water, which is allowed to equilibrate with the temperature in the shed. Although the tank also has pumps and screens for use as a flume, the flume was not used for the tests described here. When the flume is turned off the water may stratify, but profiles of temperature in these tests showed this to be a minor effect with about 1.5°C over the depth of the water in the tank. Each tow starts in stationary water but after the tow stops, the water entrained by the sensor flows over the sensor in the reverse direction and this reverse flow takes several minutes to decay to the background level.

Permanganate crystals dropped into the tank just before the sensor passes stain a vertical line in the water that reveals the distortion of the fluid by passage of the sensor. There is displacement of this line by about 2 cm at the depth of the sensor immediately after the sensor passes but there is also a continuous flow that follows the sensor down the tank at a fraction of the towing speed for several minutes. With greater stratification than in these tests, internal waves have been generated that persist for as long as 15 minutes. This was not the case here.

A choice must be made concerning mechanical penetration of the surface by some coupling element since a proper test would have the current meter being tested totally submerged yet the carriage towing the current meter must be above the water. For these tests, we elected to submerge the entire current meter and couple it to the tow carriage with a single 2" structural aluminum angle supporting a cradle to which the MAVS current meter housing was clamped. This angle generated surface waves and at high speeds ventilated to a depth of 30 cm, but we limited the speed to prevent ventilation to the depth of the sensor, which was 50 cm. Our initial measurements were made with a MAVS having a straight sensor. This required that the housing be positioned to one side of the tank to keep the sensing volume near the center. As the angle was changed, the sensor moved from the center towards the side and the housing moved into the tow direction where it created a wake that was disturbing to the sensing volume when the direction was reversed. To obtain a more accurate

measurement, the straight sensor MAVS was exchanged for a bent sensor MAVS where the housing was positioned across the tank and was rolled to change the "elevation" angle for the measurements. Fig. 5 shows the bent sensor MAVS being towed with the sensor elevation adjusted to 45°. The tow was made first to the right, stopped for 2 minutes to allow flow in the tank to decay, and then towed back to the left. Both directions were required because there is an asymmetry with the bent sensor from the sensor tube extending below the sensor and because the transducers in the plane of the support tube and the tow direction are on only the lower or proximal ring (that nearest the housing). Varying the elevation from 0° to 90° manually was accomplished by rotating the housing by a measured 5° about its long axis between tows.



Fig. 5. Bent sensor MAVS being towed with a 45° elevation angle of the sensor to the tow direction. Permanganate crystals have been dropped to streak the water in the flume so the displacement of fluid after passage of the sensor can be seen, barely visible here.

#### B. Azimuthal Results

The MAVS sensor has greatest symmetry in the plane of the rings and this is where the cosine response is essentially perfect. Fig. 6 shows a plot from a test performed at the NOAA/Great Lakes Environmental Research Laboratory [8] in a tunnel where, after the flow was established, the MAVS current meter was rotated about the axis of the sensor to detect any wake effects that might cause the response in U and V in instrument coordinates to deviate from a circle. The response was circular from 3 cm/s to 30 cm/s although the circle was offset from the origin by the uncorrected zero offset of the acoustic axes. This is a plot of horizontal cosine response as it is commonly presented.

#### C. Elevation Results

Fig. 7 shows the ratio of tow speed to the measured speed plotted against the elevation angle of the sensor. At 0° the ratio is 1.00 and this is what has been

experienced in other tests where the sensor was towed in the plane of the rings. In fact, this is experienced in any azimuthal orientation at any speed of tow from 5 cm/s to 50 cm/s. As the elevation is increased (here elevation represents the apparent angle of attack with respect to the sensor and is the inclination of the sensor tube from vertical), the ratio remains between 1.00 and 0.90 from  $-45^\circ$  to  $+30^\circ$ . However, as the elevation angle reaches  $90^\circ$  the scale factor becomes 0.80, an error of 20%.

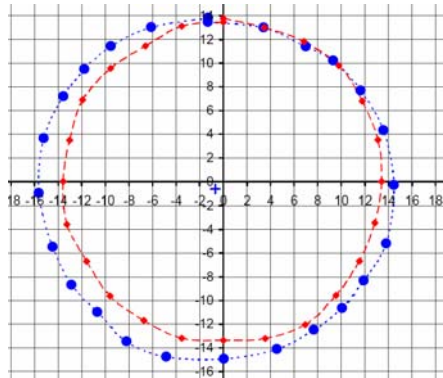


Fig. 6. Horizontal cosine response in MAVS (blue) is nearly perfect as illustrated in this propeller tunnel test done by NOAA/Great Lakes Environmental Research Laboratory [8]. The red circle is a standard used by GLERL from a SonTek ADV without structure in the flow. The offset of the blue circle from the origin is uncorrected zero offsets of the acoustic axes.

Both scale factor and error are plotted in Fig. 7 although the two displays are redundant. Scale factor is sometimes used to correct a distortion in flow produced by structure in a sensor or a non-linear response in speed. Error is generally more revealing for an uncorrected display of measurement as is the output from MAVS.

To obtain as much accuracy as possible in these elevation test runs, the temperature of the tow tank was measured and a speed of sound correction applied for each run. Speed of sound in sea-water is assumed in MAVS to be 1500 m/s and the sensors are calibrated for that. However, in fresh water at the temperatures in the flume, the speed of sound varied from 1454 to 1457 m/s and this ratio was used to correct the measurements. Measurements were recorded in the orthogonal UVW MAVS frame with U perpendicular to the plane of the bend, V across the tank and aligned with the instrument housing, and W along the axis of symmetry of the sensor, positive away from the bend. Speed was derived from the average after the start up and slow down transients were excluded. The angle of measured flow was computed as  $\arctan(W/U)$  and the error reported was the difference between this angle and the elevation angle. Elevation angle was measured by sighting the sensor support tube with a machinist's protractor to an accuracy of  $1^\circ$ .

The asymmetry between positive and negative elevation angles results from the azimuthal distribution of transducers on the two rings. Referring to Fig. 2, the transducer pairs on the ring closest to the housing (the

proximal ring) are the ones most in the wake of the distal ring for forward motion but in the clear for backward motion. Positive elevation angles are those shown for motion to the right in Fig. 5, the more disturbed direction for the acoustic transducers on the proximal ring. When the tow carriage returns backward to the left, the elevation angle is indicated as a negative angle because it is an incident flow direction below the plane of the rings. In this direction the acoustic paths are not disturbed by the wake from the distal ring. The possible disturbance from the bent support tube that extends upstream for tows in the backward direction is not detectable.

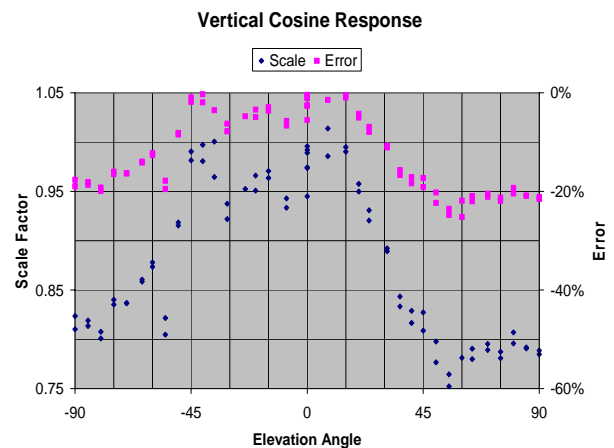


Fig. 7. Vertical cosine response of the MAVS sensor as a function of elevation angle. Scale factor is measured speed over tow speed. The error between perfect cosine response and actual cosine response is also plotted.

Speed is not the only measurement that is affected by elevation. Direction is also influenced by the elevation angle since there is lift from the faired rings that causes displacement of flow radially in the sensor frame. The effect is to make the direction align more along the sensor axis than an undisturbed measurement would be. In sensor coordinates, this is an increase in the W component of velocity, negative for positive elevation angle and forward motion, positive for positive elevation angle and backward motion. Fig. 8 shows that the angular deviation is negligible out to  $30^\circ$  of elevation and then increases to a maximum of  $10^\circ$  at  $50^\circ$  elevation, returning to  $0^\circ$  when the flow is again on axis ( $90^\circ$  elevation angle).

#### D. Speed Results

For each elevation angle in this study, the current meter was towed forward and backwards at 10 cm/s and at 30 cm/s (several more tows at  $0^\circ$  elevation were performed at 40 cm/s). Fig. 9 shows the same data as Figs. 7 and 8 sorted by speed. There is little speed effect revealed in this analysis so that at least over this speed range, there are no transitions in flow. In particular, over the elevation angle range of  $-30^\circ$  to  $+30^\circ$  the speed has no effect nor does the elevation have an effect on the angle or the measured speed.

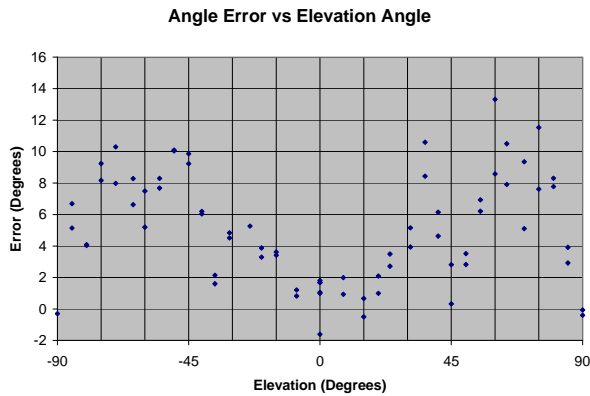


Fig. 8. Fairing of the rings steers the flow towards the axis of the sensor except when the flow is horizontal ( $0^\circ$  elevation) or vertical ( $90^\circ$  elevation).

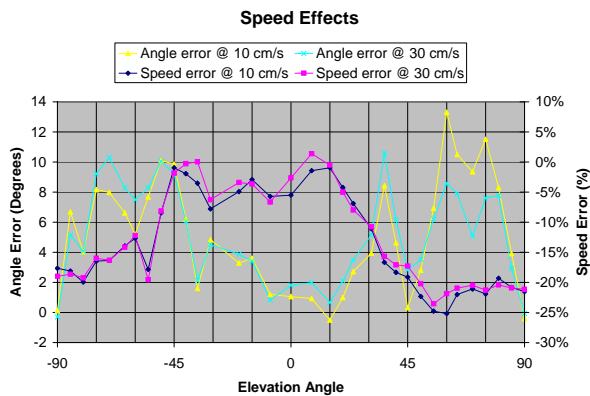


Fig. 9. Towing speed has little effect on the errors in either angle or speed.

#### IV. CONCLUSIONS

MAVS was initially designed for general purpose current measurements in clear or turbid water with or without waves, near or far from a boundary. It has been deployed from moorings, bottom tripods, AUVs, and mounted in tow tanks and in flumes for laboratory measurements. In 2002, an array of 9 MAVS current meters was mounted on a tow carriage in a civil engineering facility at Texas A&M University in a straight sensor horizontal configuration pointed into the tow direction because the velocity measurements along the sensor axis are the least disturbed by turbulence from structure. However, it was discovered that the mean velocity read low by about 18% compared to the towing speed. This was an orientation that had not been used before and it was only thought to be acceptable because of tow tests done in 1995 with a prototype sensor. Based upon the TAMU observations, the set of experiments described here were performed. One of us, S.R. Brody, did the tow tests and data analysis during a college externship in 2004.

The velocity measured with  $90^\circ$  elevation angle is indeed about 20% low, as experienced by TAMU, and this is most easily explained by the acoustic paths being shadowed by struts and by the distal ring. Even with most of the acoustic path falling in the region between struts and along a chord inside the ring, the drag of this structure moves water along with the sensor and decreases the velocity over that which would have been experienced without structure. While this is probably the worst angle for precise velocity measurements with this sensor, it is the least disturbed by turbulence and for those measurements is ideal with its high spatial resolution and rapid acquisition of fluctuations.

#### ACKNOWLEDGMENTS

This work was supported in part by Nobska Development, Inc with facilities of the Woods Hole Oceanographic Institution and the Extern Program of Swarthmore College. This is Woods Hole Oceanographic Institution contribution 11353.

#### REFERENCES

- [1] Williams, A.J. 3rd, F.T. Thwaites, and A.T. Morrison III, 1996. "Transducer supports for acoustic travel-time current meters - flow sampling, wake, and potential flow distortion considerations", *Proceedings Microstructure Sensors Workshop*, Timberline Lodge, 23-25 October 1996, pp. 38-43.
- [2] Thwaites, F.T., and A.J. Williams 3rd, 1997. "New current meter development", *Sea Technology*, April 1997, pp. 108-112.
- [3] Morrison, A. T., III, "Development of the BASS Rake acoustic current sensor: measuring velocity in the Continental Shelf wave bottom boundary layer", Ph.D. thesis, Massachusetts Institute of Technology/Woods Hole Oceanographic Institution Joint Program in Oceanographic Engineering, June 1997.
- [4] Morrison, A. T., III, "The single axis sample volume of the BASS Rake acoustic current sensor", *Proceedings OCEANS '98*, IEEE/OES, September 1998, Vol. I, pp. 239-243.
- [5] Morrison, A. T., III, Williams, A. J., 3rd, "Preliminary tow tank and flume tests of a prototype BASS Rake wave bottom boundary layer sensor", *Proceedings OCEANS '96*, MTS/IEEE/OES, September 1996, Vol. I, pp. 451-456.
- [6] Thwaites, F.T., and A.J. Williams 3rd, 1996. "Development of a Modular Acoustic Velocity Sensor", *OCEANS '96*, IEEE Catalog Number 96CH35967, pp. 607-612.
- [7] Thwaites, F.T., and A.J. Williams 3rd, 1997. "Use of tow tanks to study sensitive current meters", *OCEANS '97*, pp. 1089-1093.
- [8] <http://www.Nobska.net/> Comparisons **Flow Tank Calibration Data s13.pdf**